

Study of the performance of a large scale water-Cherenkov detector (MEMPHYS)

Luca Agostino,^a Margherita Buizza-Avanzini,^a Marcos Dracos,^b Dominique Duchesneau,^c Michela Marafini,^{a,0} Mauro Mezzetto,^d Luigi Mosca,^e Thomas Patzak,^a Alessandra Tonazzo^a and Nikolaos Vassilopoulos^{a,b}

^aAPC, Univ. Paris Diderot, CNRS/IN2P3, CEA/Irfu, Obs. de Paris, Sorbonne Paris Cité, F-75205 Paris Cedex 13, France

^bIPHC, Université de Strasbourg, CNRS/IN2P3, F-67037 Strasbourg, France

^cLAPP, Université de Savoie, CNRS/IN2P3, F-74941 Annecy-le-Vieux, France

^dINFN Sezione di Padova, I-35131 Padova, Italy

^eLaboratoire Souterrain de Modane, F-73500 Modane, France

E-mail: luca.agostino@apc.univ-paris7.fr, buizza@in2p3.fr, marcos.dracos@ires.in2p3.fr, duchesneau@lapp.in2p3.fr, michela.marafini@roma1.infn.it, mauro.mezzetto@pd.infn.it, luigi.mosca@lsm.in2p3.fr, thomas.patzak@apc.univ-paris7.fr, tonazzo@in2p3.fr, vassilo@ires.in2p3.fr

Abstract. MEMPHYS (MEgaton Mass PHYSics) is a proposed large-scale water Cherenkov experiment to be performed deep underground. It is dedicated to nucleon decay searches, neutrinos from supernovae, solar and atmospheric neutrinos, as well as neutrinos from a future Super-Beam or Beta-Beam to measure the CP violating phase in the leptonic sector and the mass hierarchy. A full simulation of the detector has been performed to evaluate its performance for beam physics. The results are given in terms of “migration matrices” of reconstructed versus true neutrino energy, taking into account all the experimental effects.

ArXiv ePrint: [1206.6665](https://arxiv.org/abs/1206.6665)

⁰Currently at Università La Sapienza, Rome, Italy

Contents

1	Introduction	1
2	The MEMPHYS detector	1
3	MEMPHYS simulation	2
4	Event selection and energy reconstruction	4
5	Migration matrices	7
6	Conclusions	10

1 Introduction

A megaton-scale water Cherenkov detector would have competitive capabilities for accelerator-based neutrino oscillation physics. In addition, it would reach a sensitivity on the proton lifetime close to the predictions of most supersymmetric or higher dimension grand unified theories and it would explore neutrinos from supernovae and from other astrophysical sources.

Such a detector is most attractive because it relies on a well established technique, already used by the IMB [1], KamiokaNDE [2] and SuperKamiokande [3] (SK) experiments. Each tank will be roughly 10 times the size of SK, a reasonable extension of a known, well performing detector.

An expression of interest for such a project, called MEMPHYS (MEgaton Mass PHYSics), was prepared [4].

The potential for neutrino physics with specific Super-Beams and Beta-Beams at the Fréjus site was investigated in detail in [5]. The authors assumed the same performance as the SK detector in terms of detection efficiency, particle identification capabilities and background rejection. The behaviour of a larger scale detector will, however, be different, because of the larger distance traveled by light to reach the photomultipliers.

In this paper, a realistic evaluation of the expected MEMPHYS performance is presented. It is based on a full simulation and complete reconstruction and analysis algorithms. “Migration matrices” from true to reconstructed neutrino energy are provided.

2 The MEMPHYS detector

MEMPHYS is a proposed large-scale water Cherenkov detector with a fiducial mass of the order of half a megaton.

The detector could be installed at the Fréjus site, near the existing *Laboratoire Souterrain de Modane* (LSM laboratory), in the tunnel connecting France to Italy, located at 130 km from CERN and with a rock overburden of 4800 m.w.e. Possible installation at other European sites was studied in the context of the LAGUNA EU-FP7 Design Study [6].

The original plan [4] envisaged 3 cylindrical detector modules of 65 meters in diameter and 60 meters in height. At the Fréjus site, the characteristics of the rock allow for a larger excavation in the vertical direction. Heights up to 103 m are possible, which would allow

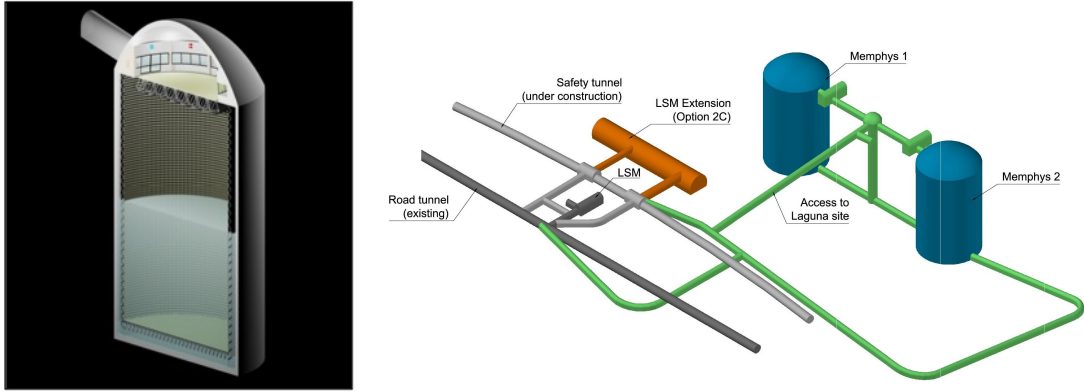


Figure 1. Schematic view of one MEMPHYS module (left) and design for installation and infrastructure at a possible extension of the LSM underground laboratory at the Fréjus site (right). Each tank is 65 m in diameter and 103 m in height. The total fiducial mass is 500 kton.

for the same total fiducial mass with only two modules. The latest design [7] envisages 2 modules of 103 m height and 65 m diameter. Taking into account a 1.5 m thick veto volume surrounding the main tank and a cut at 2 m from the inner tank wall for the definition of the fiducial volume, as done in SK to allow for Cherenkov cone development, the total fiducial mass would be 500 kilotons.

Each module is equipped with ~ 120000 8" or 10" photomultipliers (PMTs) providing 30% optical coverage (equivalent, in terms of number of collected photoelectrons, to the 40% coverage with 20" PMTs of SK).

A schematic view of the detector and of a possible layout for installation at the Fréjus site are shown in figure 1.¹

3 MEMPHYS simulation

In order to evaluate realistic performance for the above-described baseline detector, a detailed simulation has been developed, mainly in the context of the EUROnu FP7 Design Study [8]. The code, based on the Geant-4 toolkit [9, 10], was originally written for the T2K-2km detector [11], then interfaced with the OpenScientist framework [12]. It allows for interactive event viewing, batch processing and analysis. Special care has been devoted to the modularity of the code in the definition of the detector geometry, to facilitate future detector optimisation studies. The GENIE [13] event generator is used for neutrino interactions.

The model implemented in Geant-4 for light propagation in water includes the effects of Rayleigh scattering, Compton scattering and absorption. The attenuation length thus obtained is very similar to the one shown by the SK Collaboration [14], providing evidence for the reliability of the simulation.

One basic quantity used to evaluate the detector performance is the number of photoelectrons (PEs) per MeV as a function of the particle energy. This is shown in figure 2(a), for electrons generated uniformly in the detector volume. The number of PEs per MeV is about constant and equal to 11 for energies above 5 MeV. Figure 2(b) shows the number

¹Courtesy of Lombardi Engineering S.A.

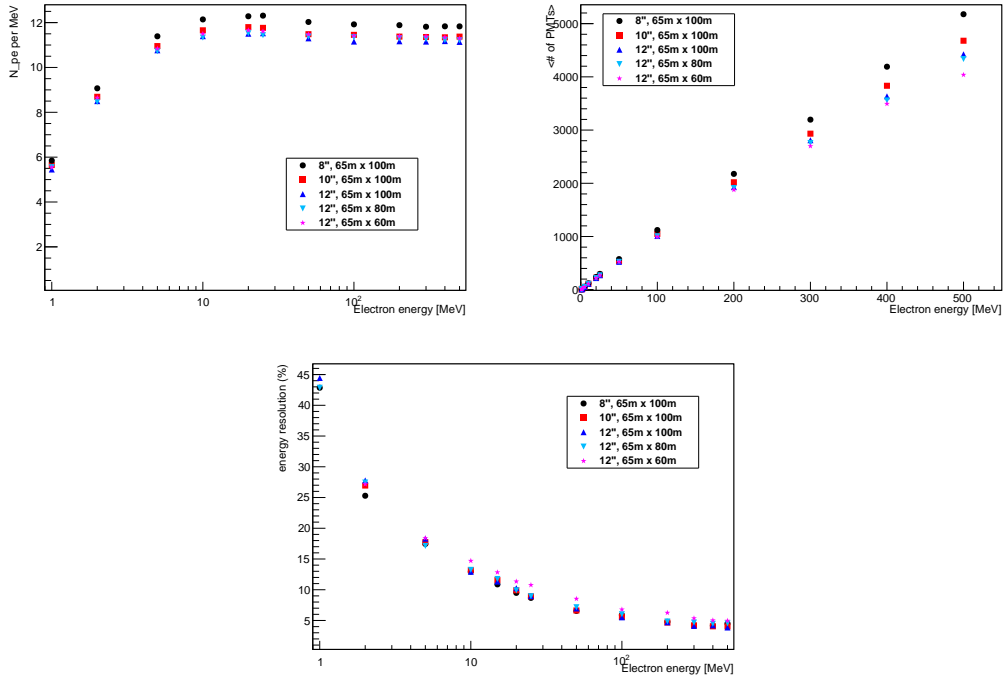


Figure 2. Detector response for different tank heights (60, 80 and 100m) and PMT sizes (8", 10" and 12"). Top left: Number of detected photoelectrons per MeV as a function of electron energy. Top right: Number of PMTs with at least one photoelectron as a function of electron energy. Bottom: Momentum resolution as a function of electron energy.

of hit PMTs as a function of energy. The resolution on the estimated electron momentum, evaluated as explained below, is shown in Figure 2(c).

As can be seen from the figures, these quantities are very weakly affected by the tank height, thus we can conclude that this parameter has no significant impact on the detector's performance. The new baseline configuration, with 2 tanks of 65 m diameter and 103 m height, is used in the following.

The response is also nearly unaffected by PMT size. For the simulation presented here, 12" PMTs were actually used: they provide identical response to 10" PMTs and only slight differences with respect to 8" PMTs.

The impact of PMT noise on beam neutrino physics is not expected to be a major issue. With a dark count rate of 7 kHz per PMT and an event hit integration time of 50 ns, the number of spurious hits per event will be of the order of 40, much smaller than our threshold on the minimum number of hits for event reconstruction (500 hits, corresponding to about 50 MeV of reconstructed electron momentum). The use of a 50 ns integration window, as in SK, is justified by the distribution of the PMT hit time residuals with respect to the reconstructed vertex, shown in Figure 3: the large majority of the hits lie within this range. PMT noise was however implemented in the simulation, and its impact was evaluated on some features of the analysis, as explained below.

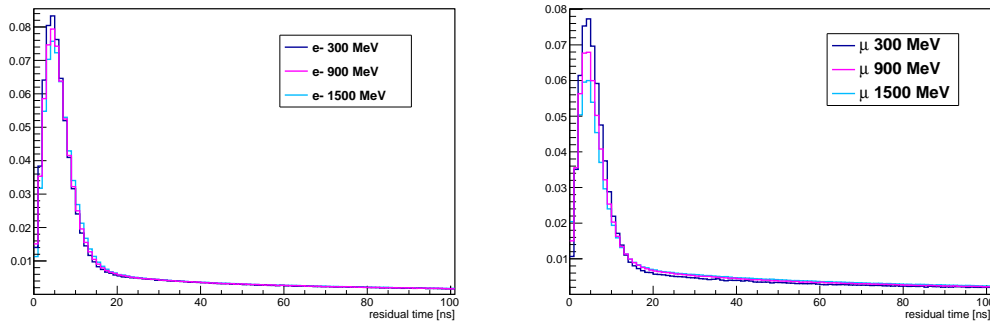


Figure 3. Distribution of the PMTs residual times with respect to the reconstructed vertex, for electrons (left) and muons (right) of different energies.

4 Event selection and energy reconstruction

A complete analysis chain has been developed, based on what is done in SK [15]. Some of the algorithms are a simplified version of those of SK. Their performance was also evaluated by running the full simulation with the SK parameters (size, PMT coverage etc.) to ensure that no significant degradation of efficiencies and background rejection are introduced by our algorithms. A rescaling was then applied to account for the small differences due to our simplifications.

The aim of the analysis is the reconstruction of the incoming neutrino energy and the identification of its flavour, to perform appearance or disappearance measurements with different types of beams. This is only relevant for Charged Current (CC) neutrino interactions. Neutral Current (NC) interactions where a final-state pion can mimic an electron or muon are considered separately.

The analysis proceeds through the following steps:

- reconstruction of the interaction vertex, from the timing of the hits in the different PMTs;
- determination of the outgoing lepton direction, from the pattern of the Cherenkov ring;
- lepton identification, from the “fuzziness” of the Cherenkov ring: since electrons are more subject to bremsstrahlung and multiple scattering, they produce rings whose edge is less “sharp” than in those of muons. A simplified particle identification algorithm is used, considering the fraction of charge inside the edge of the ring;
- rejection of NC interaction with a π^0 in the final state, which can mimic an electron (more details are given below);
- reconstruction of the lepton momentum, from the measured charge in the PMTs;
- finally, determination of the incoming neutrino energy.

One of the most severe backgrounds in the search for ν_e appearance is due to NC events with a π^0 in the final state: the two γ 's originating from its decay produce rings similar to those of electrons, and the rejection of these events is mainly based on the reconstruction of a second ring in an electron-like event. Figure 4 shows examples of a single-ring (electron)

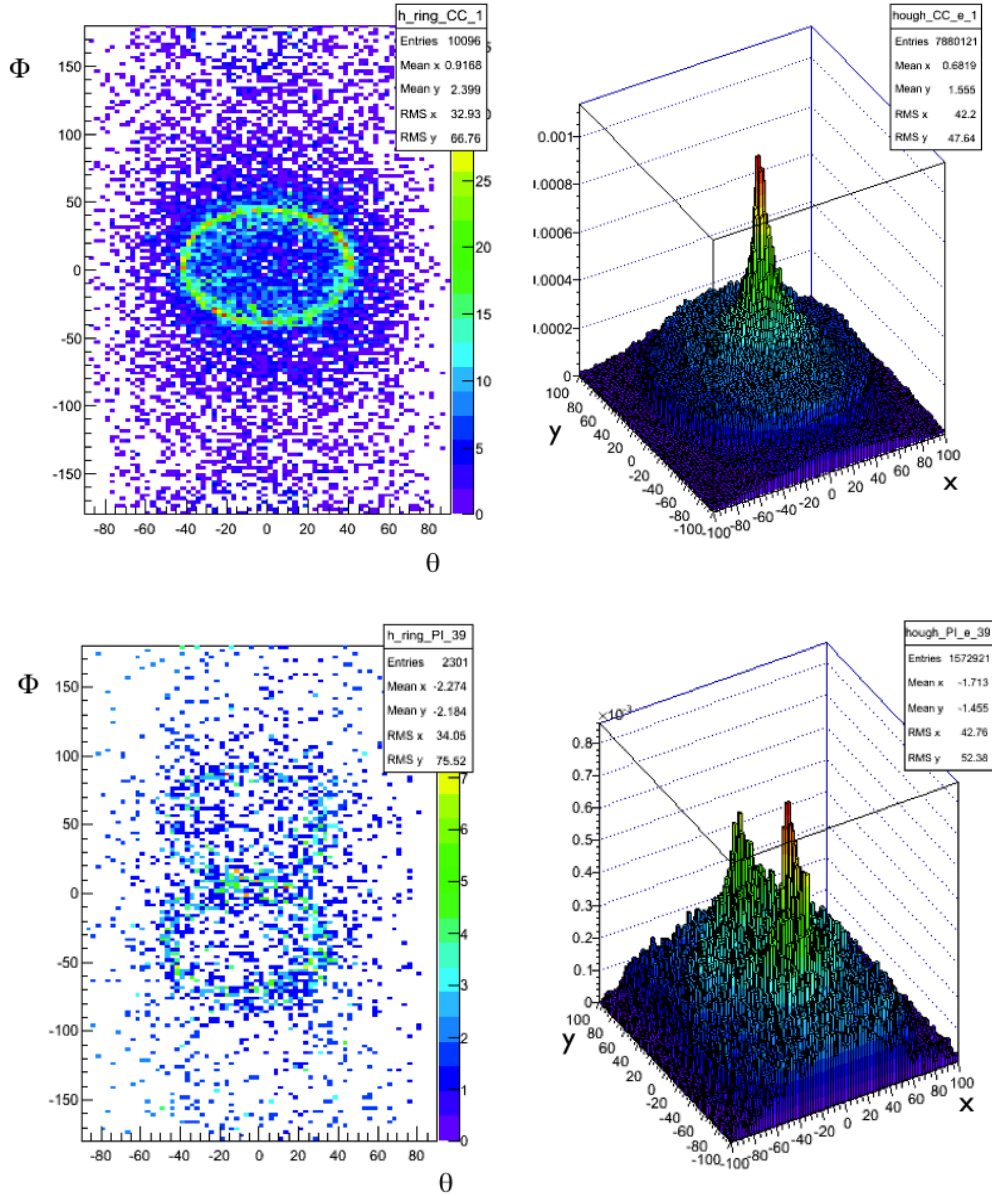


Figure 4. Single ring (top) and double ring (bottom) events: projection in spherical coordinates centered on the reconstructed vertex and direction (left) and their Hough transform (right).

and a double-ring (π^0) event: the rings are first projected in spherical coordinates centered on the fitted particle vertex and direction, then Hough-transformed [16] to peaks for automated counting. The π^0 identification algorithm used in this analysis is much simplified with respect to the one used in SK and in the HyperKamiokande LOI [17]: in particular, we don't implement a cut on the invariant mass of two rings, when a second ring is forced to be found. We have applied our π^0 identification algorithm selection on a sample of neutrinos interacting in a detector simulated with an approximate SK geometry (40 m diameter, 40 m height, 40% optical coverage with 20" PMTs), and we have found a π^0 contamination very

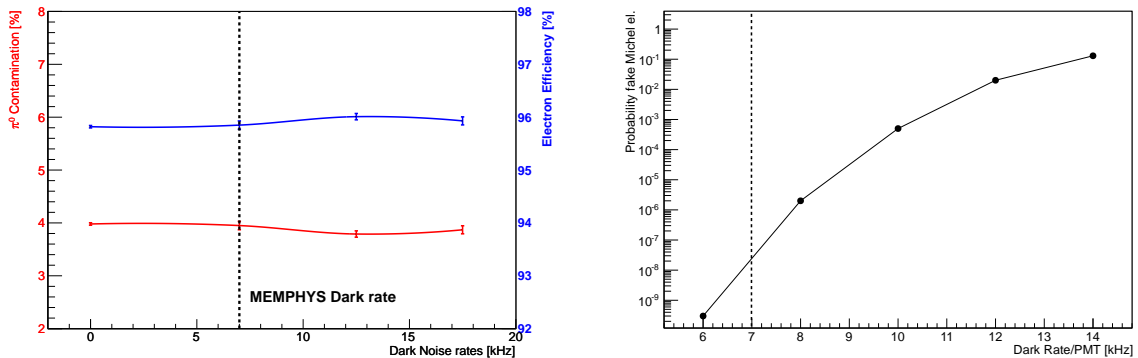


Figure 5. Study of the impact of PMT dark noise on the analysis. Left: π^0 contamination and efficiency for ν_e -CC identification as a function of dark count rate per PMT. Right: probability of finding a fake Michel-electron as a function of dark count rate per PMT. A dark count rate of about 7 kHz per PMT, shown by the vertical lines, is considered as a realistic estimate for the MEMPHYS detector.

similar to what we find with the MEMPHYS simulation, namely 3.9%: this suggests that we can assume the efficiency of the selection to be nearly independent of the detector size. The efficiencies of the π^0 rejection cut were rescaled to those of [17], considering that we will eventually implement their full likelihood analysis and cuts. A cut on the Michel electron from muon decay was also implemented; this cut introduces some differences between muon neutrino and anti-neutrino identification efficiency, and in addition suppresses completely the ν_e contamination in the ν_μ sample.

PMT dark noise could in principle affect the analysis by worsening the performance of selection cuts where a small number of hits can have a significant impact. One example is the selection of π^0 s, where the second ring can be faint. Another one is the tagging of Michel electrons following muon decays, as noise hits can mimic a low energy electron after ν_e -CC events and thus reduce the efficiency for their identification or increment their contribution to the background of the ν_μ -CC sample. PMT noise was implemented in the simulation in order to evaluate its impact, in particular on these two cuts. The efficiency for single-ring identification and the π^0 contamination in ν_e -CC events were evaluated as a function of PMT dark rate, and found to be quite insensitive to it, as shown in Figure 5 (left). The probability to tag a fake Michel electron is shown as a function of dark count rate in Figure 5 (right), and is extremely low for the dark count rate expected in MEMPHYS. We can conclude that no significant degradation of the analysis performance should be expected from PMT dark noise.

The incident neutrino energy is deduced from the measured lepton momentum and direction, assuming the interaction to be CC and quasi-elastic (QE). In a pure 2-body collision $\nu_l + N \rightarrow l + N'$ (where $l=e$ or μ and N denotes a nucleon, either p or n), and assuming the nucleon is at rest, the incoming neutrino energy E_ν is related by simple kinematics to the outgoing lepton energy E_l and momentum P_l and to the angle θ_l of the lepton direction with respect to the neutrino:

$$E_\nu = \frac{m_N E_l - m_l^2/2}{m_N - E_l + P_l \cos \theta_l} \quad (4.1)$$

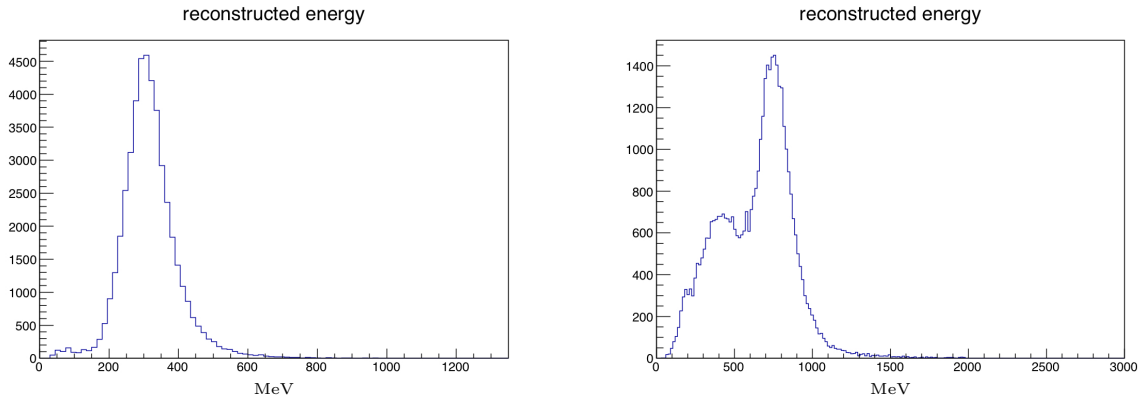


Figure 6. Reconstructed energy for selected muon neutrinos with energies of 360 MeV (left) and 840 MeV (right).

The difference between the reconstructed and true neutrino energy in two different energy ranges is shown in figure 6: the Gaussian peak is due to true QE interactions, with a smearing induced by the Fermi motion of the nucleon and the experimental resolution, while the tail at lower reconstructed energies is due to non-QE interactions, whose contribution is larger as the neutrino energy increases.

5 Migration matrices

In order to properly take into account all the effects of the reconstruction, the detector performance is conventionally described in terms of “migration matrices” representing the reconstructed neutrino energy as a function of the true one. Each “slice” of true energy is normalized such that the projection of the matrix corresponds to the efficiency for the given neutrino energy. Separate matrices are constructed for signal and background in the different detection channels, and for CC and NC events.

Events identified as electron neutrinos are the signal in the appearance channel in a “traditional” neutrino beam (Super-Beam) [18], composed mainly of ν_μ ’s, where the oscillation $\nu_\mu \rightarrow \nu_e$ is searched. Separate migration matrices are provided for CC and NC interactions. The background is given by mis-identified ν_μ CC interactions as well as by other components present in the beam in small fraction (mainly ν_e ’s and anti-neutrinos; no detailed study has been performed here for ν_τ ’s, since the beam energy is below the threshold for τ production). Events identified as muons are the signal for the appearance channel $\nu_e \rightarrow \nu_\mu$ with a Beta-Beam [19, 20] or for the disappearance channel $\nu_\mu \rightarrow \nu_\mu$ with a Super-Beam.

The details of the matrices are provided in figure 7. The efficiencies as a function of neutrino energy are shown in figure 8.

Examples of neutrino and antineutrino spectra measured in the MEMPHYS detector are shown in Figure 9. They are obtained with the Super-Beam fluxes provided by A.Longhin [18], from CERN to the Fréjus site, and using the migration matrices to account for experimental effects.

The matrices are available from the authors in the text format suitable as input for the GLOBES package [21, 22].

Figure 10 shows an example of study of sensitivity to the leptonic CP violation phase using the GLOBES package, with a Beta-Beam [5] and a Super-Beam [18] from CERN to

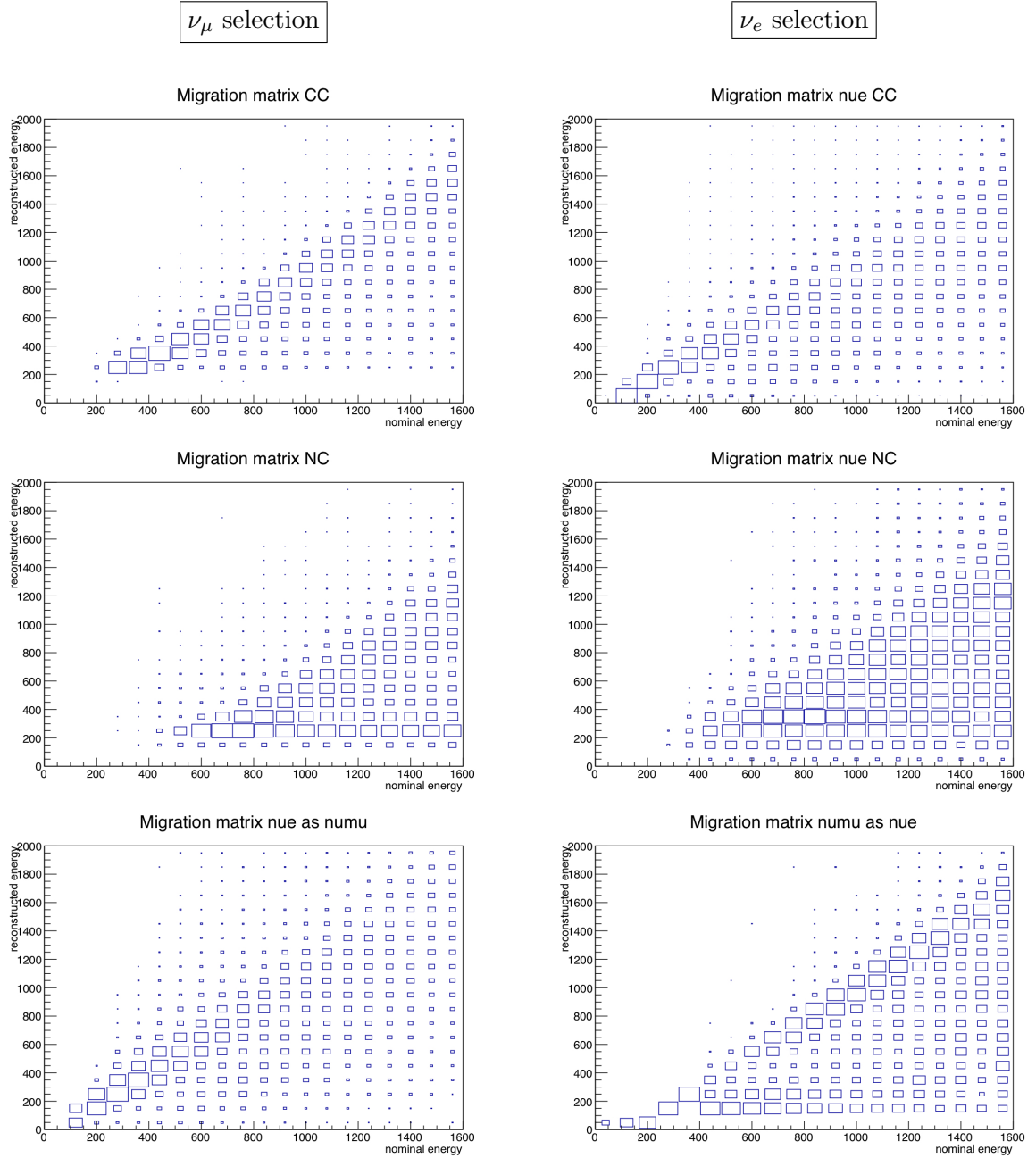


Figure 7. “Migration matrices” with reconstructed neutrino energy as a function of true energy for selected events. Left: events identified as muon neutrinos, when they are ν_μ CC interactions (top), NC interactions (middle), ν_e CC interactions (bottom). Right: events identified as electron neutrinos, when they are ν_e CC interactions (top), NC interactions (middle), ν_μ CC interactions (bottom).

Fréjus. For the Beta-Beam, a running time of 5 years with neutrinos and 5 years with antineutrinos is considered, with a systematic uncertainty of 2% on both signal and background. For the Super-Beam, a running time of 2 years with neutrinos and 8 years with antineutrinos is considered, with a systematic uncertainty of 5% on signal and 10% on background. Normal mass hierarchy is assumed. The sensitivity to the CP violation phase in the leptonic sector,

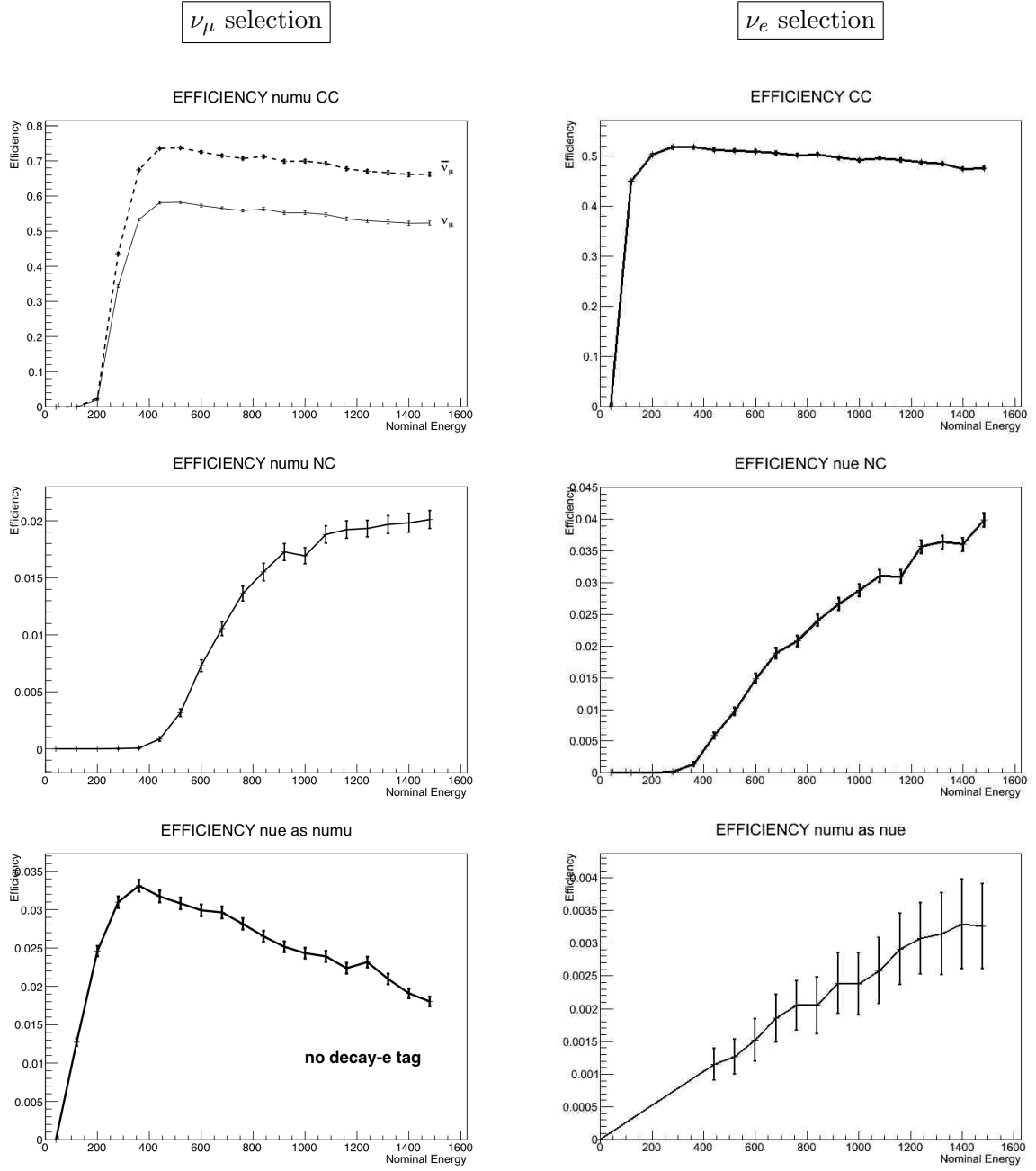


Figure 8. Efficiencies for the selection of the different neutrino event categories in the MEMPHYS detector, as a function of neutrino energy. Left: events identified as muon neutrinos, when they are ν_μ CC interactions (top), NC interactions (middle), ν_e CC interactions (bottom. The cut decay-electron tag completely suppresses ν_e CC interactions and has not been applied for this plot). Right: events identified as electron neutrinos, when they are ν_e CC interactions (top), NC interactions (middle), ν_μ CC interactions (bottom).

δ_{CP} , is shown, at 3σ and 5σ , as a function of the θ_{13} mixing angle.

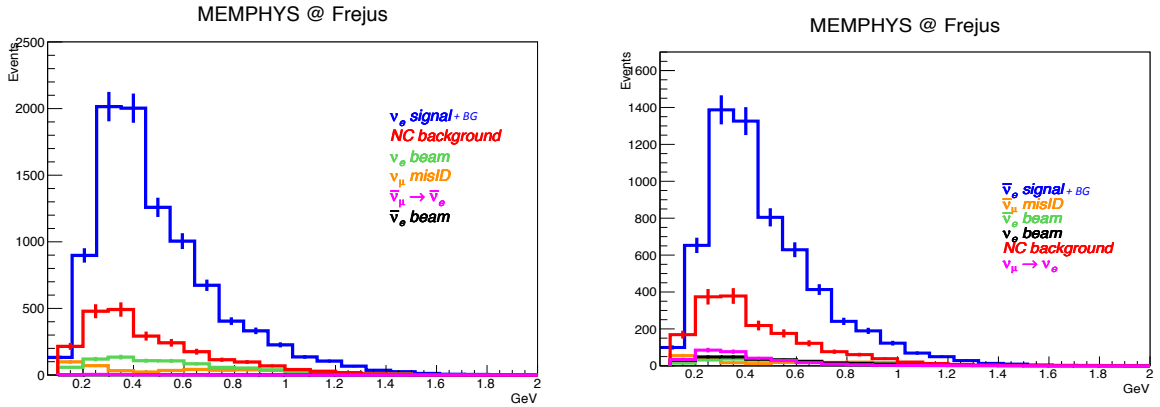


Figure 9. Neutrino (left) and antineutrino (right) spectra measured in MEMPHYS with a Super-Beams from CERN to the Fréjus site, obtained with our migration matrices. The running time is 2 years and 8 years respectively. $\sin^2 2\theta_{13} = 0.1$ and $\delta_{CP} = 0$ are assumed.

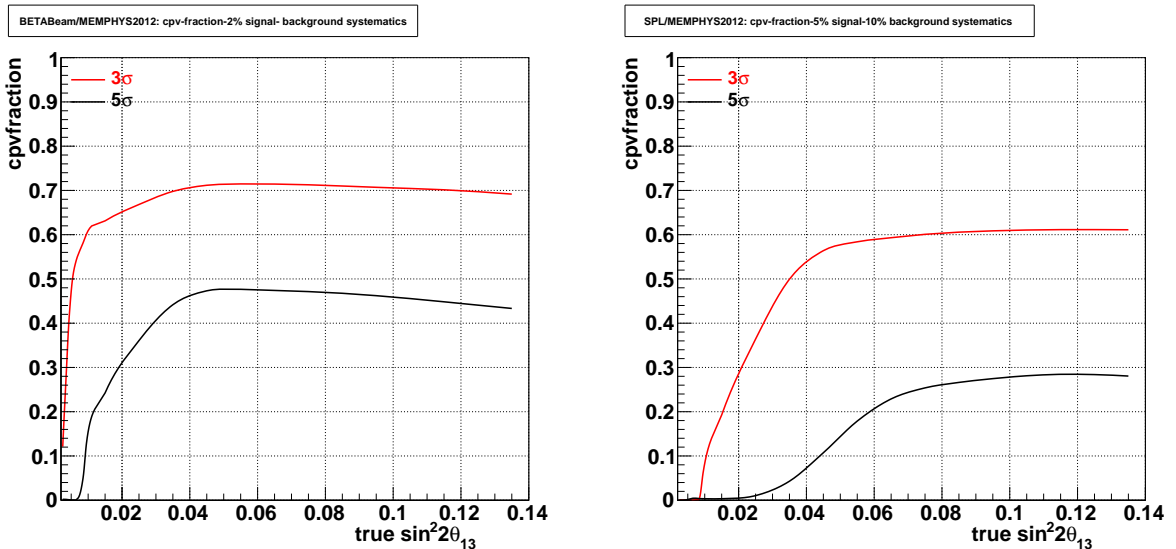


Figure 10. Example of study of sensitivity to the leptonic CP violation phase using the GLOBES package, considering a Beta-Beam (left) or a Super-Beam (right) from CERN to the Fréjus site.

6 Conclusions

A detailed study of the performance of a future large-scale water-Cherenkov detector, MEMPHYS, has been performed, using a full simulation of the detector's response and realistic analysis algorithms. The results have been presented in terms of migration matrices from true to reconstructed neutrino energy, considering the signal and background channels for different neutrino beam types.

Acknowledgments

We are grateful to Enrique Fernandez Martinez, Pilar Coloma and Sanjib Agarwalla for useful discussion. We acknowledge the financial support of the European Community under

the European Commission Framework Programme 7 Design Study EUROnu, Project Number 212372 and Design Study LAGUNA-LBNO, Project Number 284518. The EC is not liable for any use that may be made of the information contained herein.

References

- [1] **IMB** Collaboration, C. Bratton et al. *Phys. Rev. D* **37** (1988) 3361.
- [2] **KamiokaNDE** Collaboration, M. Koshiba et al. *Nuovo Cim.* **C9** (1986) 141–158.
- [3] **Super-Kamiokande** Collaboration, S. Fukuda et al. *Nucl. Instrum. Meth.* **A501** (2003) 418.
- [4] A. de Bellefon, J. Bouchez, J. Busto, J.-E. Campagne, C. Cavata, et al., *MEMPHYS: A Large scale water Cherenkov detector at Frejus*, [hep-ex/0607026](#).
- [5] J.-E. Campagne, M. Maltoni, M. Mezzetto, and T. Schwetz, *Physics potential of the CERN-MEMPHYS neutrino oscillation project*, *JHEP* **0704** (2007) 003, [[hep-ph/0603172](#)].
- [6] **LAGUNA** Collaboration, T. Patzak et al., *LAGUNA: Future megaton detectors in europe*, *J.Phys.Conf.Ser.* **309** (2011) 012022.
- [7] J. Borne, J. Busto, J. Campagne, M. Dracos, C. Cavata, et al., *The MEMPHYS project*, *Nucl.Instrum.Meth.* **A639** (2011) 287–289.
- [8] <http://www.euronu.org/>.
- [9] **GEANT4** Collaboration, S. Agostinelli et al., *GEANT4: A Simulation toolkit*, *Nucl.Instrum.Meth.* **A506** (2003) 250–303.
- [10] J. Allison, K. Amako, J. Apostolakis, H. Araujo, P. Dubois, et al., *Geant4 developments and applications*, *IEEE Trans.Nucl.Sci.* **53** (2006) 270.
- [11] M. Fechner. personal communication, 2007.
- [12] G. Barrand. personal communication, 2007.
- [13] C. Andreopoulos, A. Bell, D. Bhattacharya, F. Cavanna, J. Dobson, et al., *The GENIE Neutrino Monte Carlo Generator*, *Nucl.Instrum.Meth.* **A614** (2010) 87–104, [[arXiv:0905.2517](#)].
- [14] **Super-Kamiokande** Collaboration, K. Abe et al., *Solar neutrino results in Super-Kamiokande-III*, *Phys.Rev.* **D83** (2011) 052010, [[arXiv:1010.0118](#)].
- [15] **Super-Kamiokande** Collaboration, M. Shiozawa, *Reconstruction algorithms in the Super-Kamiokande large water Cherenkov detector*, *Nucl.Instrum.Meth.* **A433** (1999) 240–246.
- [16] E. R. Davies, *Machine Vision: Theory, Algorithms, Practicalities*. Academic Press, San Diego, 1997.
- [17] K. Abe, T. Abe, H. Aihara, Y. Fukuda, Y. Hayato, et al., *Letter of Intent: The Hyper-Kamiokande Experiment — Detector Design and Physics Potential —*, [[arXiv:1109.3262](#)].
- [18] A. Longhin, *A new design for the CERN-Fréjus neutrino Super Beam*, *Eur.Phys.J.* **C71** (2011) 1745, [[arXiv:1106.1096](#)].
- [19] P. Zucchelli, *A novel concept for a anti- ν/e / ν/e neutrino factory: The beta beam*, *Phys.Lett.* **B532** (2002) 166–172.
- [20] M. Lindroos and M. Mezzetto, *Beta Beams*. Imperial College Press, 2010.
- [21] P. Huber, M. Lindner, and W. Winter, *Simulation of long-baseline neutrino oscillation experiments with GLOBES (General Long Baseline Experiment Simulator)*, *Comput.Phys.Commun.* **167** (2005) 195, [[hep-ph/0407333](#)].

- [22] P. Huber, J. Kopp, M. Lindner, M. Rolinec, and W. Winter, *New features in the simulation of neutrino oscillation experiments with GLOBES 3.0: General Long Baseline Experiment Simulator*, *Comput.Phys.Commun.* **177** (2007) 432–438, [[hep-ph/0701187](#)].